



Genetic Types of the tp12cx Strike-Slip Fault Segments and Their Role in Controlling Reservoirs in the Tarim Basin

Yanping Lv, Hailong Ma*, Zhen Wang, Guangxiao Deng and Huan Wen

Sinopec Northwest Oilfield Company, Urumqi, China

OPEN ACCESS

Edited by:

Hu Li,
Southwest Petroleum University,
China

Reviewed by:

Jianhua He,
Chengdu University of Technology,
China
Heng Zhang,
China University of Geosciences
Wuhan, China

*Correspondence:

Hailong Ma
297048455@qq.com

Specialty section:

This article was submitted to
Economic Geology,
a section of the journal
Frontiers in Earth Science

Received: 09 April 2022

Accepted: 02 May 2022

Published: 01 June 2022

Citation:

Lv Y, Ma H, Wang Z, Deng G and
Wen H (2022) Genetic Types of the
tp12cx Strike-Slip Fault Segments and
Their Role in Controlling Reservoirs in
the Tarim Basin.
Front. Earth Sci. 10:916475.
doi: 10.3389/feart.2022.916475

The change of motion mode of multistage active strike-slip faults controls the segmentary types of strike-slip faults, which is seldom studied. Based on high-precision 3D seismic data and the principle of structural analysis, this paper defines the structural evolution characteristics of the tp12cx strike-slip fault in the key structural period and identifies the fault segmentation types. Combined with the statistical results of drilling production data and fault width, it is demonstrated that different fault segments display various reservoir architecture and hydrocarbon potential. The tp12cx strike-slip fault experienced two phases of tectonic activity controlling reservoir development: the middle Caledonian and the late Caledonian to early Hercynian. During the middle Caledonian period, a left-lateral and left-step strike-slip fault was formed. The overlapping segments of the left steps were transtension zones, and the rest were pure strike-slip segments. From the late Caledonian to the early Hercynian, the movement mode changed from left-lateral to right-lateral, and the arrangement of left steps remained unchanged, forming right-lateral and left-step strike-slip faults. That is, as a weak zone, the transtension zones of all the preexisting overlapping segments took the lead in moving into many pure strike-slip segments and maintained the transtensional property. During the right-lateral slipping process of all the original pure strike-slip segments along the fault, they were blocked and squeezed by the surrounding rocks on both sides, forming a series of “positive” flower-shaped fault anticlines, which became overlapping segments, and the fault property became transpressional. Under the continuous action of the right-lateral slipping, a regional right-lateral and right-step strike slip fault formed. The interiors of the right-step-arranged faults were composed of the left-step arranged faults. Among them, the right-step overlapping segments were weakly step overlapping segments were weakly transtensional, and the larger the fault width of the internal left step pure strike slip and overlapping segments, the stronger the dissolution. The deformation of the right-step pure strike-slip segments was weak and basically maintained the characteristics of the previous stage. According to the evolution and superposition of pure strike-slipped and overlapped segments and the changes in fault properties, four types of strike-slip fault segments and corresponding reservoir models are divided. Type I: left-step pure strike-slip segment + left-step transpressional segment + right-step transtensional segment; Type II: left-step

transtensional segment + left-step pure strike-slip segment + right-step transtensional segment; Type III: left-step pure strike-slip segment + left-step transpressional segment; and Type IV: left-step transtensional segment + left-step pure strike-slip segment. The fault width and oil production of type II and type IV with transtensional properties are much larger than those of type I and type III with transpressional properties.

Keywords: strike-slip fault, structural evolution, fault segment type, movement mode, reservoir mode

INTRODUCTION

Petroleum exploration in the Tabei Tazhong area of the Tarim Basin in China shows that strike-slip faults not only are important oil migration pathways but also play an important role in controlling the development of fractured vuggy reservoirs in carbonate karst and hydrocarbon accumulation (Deng et al., 2018; Lu et al., 2018; Qiu et al., 2019; Deng et al., 2021; Zhang et al., 2021). The control of carbonate reservoirs by strike-slip faults is mainly reflected in the following aspects: first, fault activity creates a certain range of fracture zones, and many fractures near the fault surface improve reservoir quality (Stefanov and Bakeev, 2014; Lu et al., 2017; Ramadhan et al., 2018; Neng et al., 2018; Zhao et al., 2020; Jiang et al., 2020). second, the network channel formed by faults is conducive to atmospheric freshwater leaching and deep hydrothermal fluid corrosion transformation of the fracture network and surrounding rock, thus forming a large number of corrosion holes (Lu et al., 2017; Yin et al., 2019; Yin et al., 2018b; Li et al., 2019; Li et al., 2020; Li, 2022). A strong-amplitude seismic reflection anomaly is well matched with the fault development area, which indicates that the fault transformation area is the dominant area for the development of dissolution pores (Li et al., 2020; Zhao et al., 2020). A strike-slip fault is composed of multiple pure strike-slip segments and overlapping segments, which can be divided into two types: transpressional and transtensional (Yin et al., 2019; Yin et al., 2020). The left-step overlapping segments of a left-lateral strike-slip fault or the right-step overlapping segments of a right-lateral strike-slip fault are in a state of transtensional stress and develop tension and fault depressions. the right-step segments of a left-lateral strike-slip fault or the left-step segments of a right-lateral strike-slip fault are in a state of compressive stress and develop transpression and fault uplift (Aydin and Nur, 1985; Wang et al., 1999; McClay et al., 2001; Cunningham et al., 2007). An transtensional fault has an oblivious effect on fluid migration. In particular, a strike-slip fault overlapping a transtensional segment reservoir is well developed, and oil are enriched (Stefanov and Bakeev, 2014; Deng et al., 2020; Fan et al., 2020). The segmentation of strike-slip faults is of great importance to the deployment of development plans, the construction of well patterns and the selection of drilling technology (Lu et al., 2017; Qie et al., 2021; Shan et al., 2021).

In addition to the differences between structural styles and stress states, the relationship between faults and reservoirs is also considered (Li et al., 2018; Ma et al., 2019; Li et al., 2021; Yin et al., 2019; Yin et al., 2020; Zhou et al., 2022). However, due to the vertical dip angle, small fault distance and narrow deformation zone

of a small-scale strike-slip fault, it is difficult to restore the fault style and evolution characteristics of each stage due to the high degree of fracturing in the narrow fault zone, complex structure and accuracy of seismic data identification (He et al., 2020; Zheng et al., 2020; Chen et al., 2021; Zhao et al., 2021; Lan et al., 2021; Zhu et al., 2022; Liu et al., 2022). Changes in the stress state and movement mode of multistage strike-slip faults lead to changes in the fault style, nature, width and quantity (de Jossineau and Aydin, 2007; Mitchell et al., 2009; Kim et al., 2003; Chemenda et al., 2016; Davis et al., 2000; Dooley et al., 2012; Swanson, 2005; Yin and Ding, 2019) and control the reservoir scale and distribution. In the Tabei area, a NE strike-slip fault in the oil enrichment zone has not yet been restored, and the pattern of changes in structural style and its reservoir control function in the key structural period have not been determined. This would be helpful to the further study and understanding of the mechanism of multistage strike-slip faults controlling reservoirs in the Tabei area. The changes in structural style and reservoir control during the key structural period of NE strike-slip fault restoration in the oil enrichment zone in the Tabei area need to be further studied.

In this paper, using high-precision 3D seismic data and structural analysis methods, the NE-trending tp12cx strike-slip fault in the Tabei area is optimized. Combining this information with the regional geological background, the changes in the fault movement mode and structural style in the key tectonic period are reconstructed, and the fault genetic segmentation types are established. The fault properties, width, reservoir development scale, oil production, analysis of reservoir control, and reservoir control are determined. An oil enrichment model corresponding to the genetic segment types of the tp12cx strike-slip fault is established. This study is expected to provide a certain guiding importance for the exploration and development of karst fracture cave reservoirs related to strike-slip faults.

GEOLOGICAL SETTINGS

The large NE-trending tp12cx strike-slip fault is located in the Tabei uplift of the Tarim Basin (**Figure 1**). The planar length of the 3D seismic study area is 67 km (actually more than 88 km), and NW-trending strike-slip faults form multiple groups of “X”-type conjugate faults in map view. By the end of 2020, the fault zone had accumulated oil production of 12.64 million tons, accumulated water production of 1.31 million tons, and average oil production of a single well of 87000 tons. This area is one of the most important oil production reservoirs in the Middle and Lower Ordovician. Its burial depth is more than 6000 m, indicating deep-ultradeep oil exploration. The strata in the study area are well developed, including the Sinian, Cambrian, Ordovician, Silurian, Devonian,

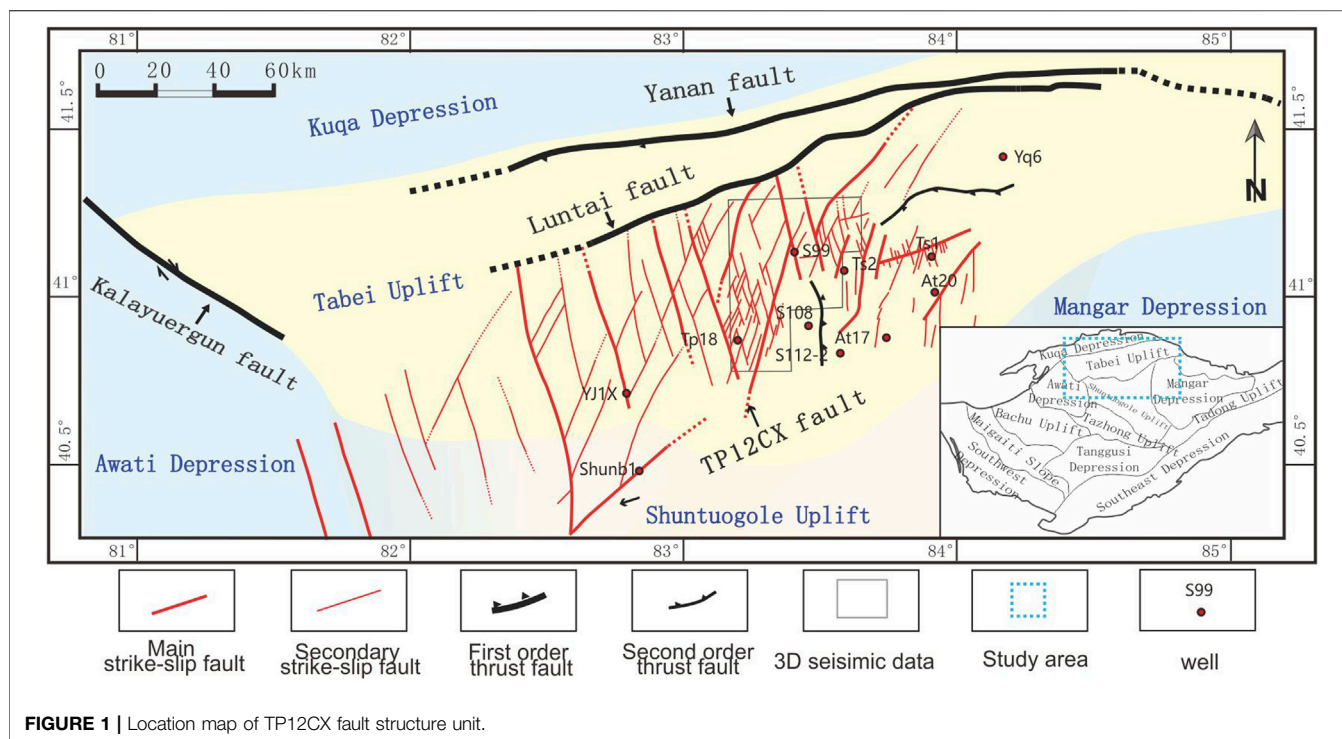


FIGURE 1 | Location map of TP12CX fault structure unit.

Carboniferous, Permian, Triassic, Jurassic, Cretaceous, Paleogene, Neogene and Quaternary systems. The Ordovician system can be subdivided into the upper Sangtamu Formation (O_{3s}), Lianglitage Formation (O_{3l}) and Qiarbak Formation (O_{3q}) from top to bottom. The middle Yijianfang Formation (O_{2yj}), the middle to lower Yingshan Formation (O_{1-2y}), and the lower Ordovician Penglaiba Formation (O_{1p}). From south to north, the Sangtamu Formation and Lianglitage Formation were eroded and pinched out (Figure 2).

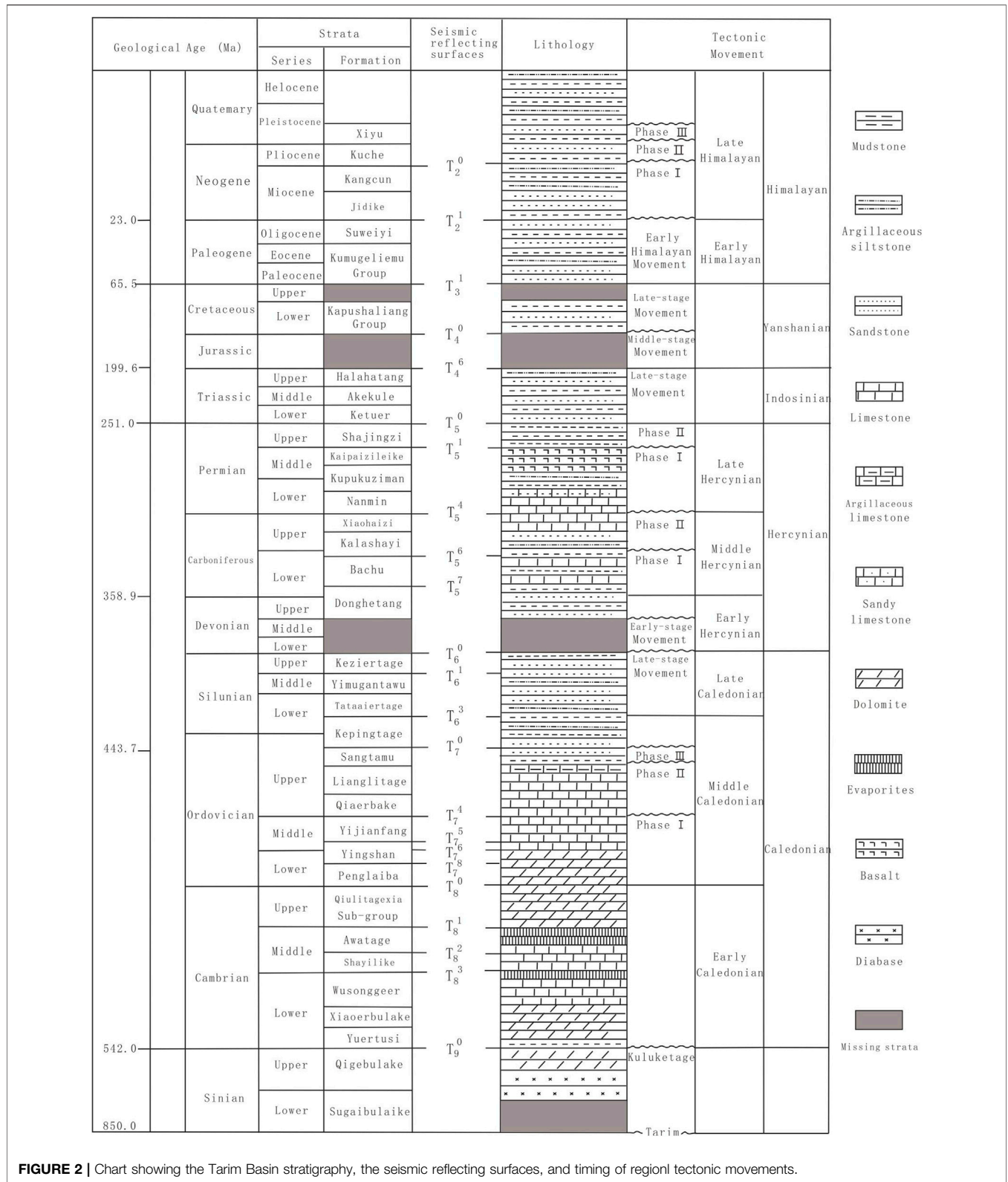
The study area underwent multiple main tectonic episodes, including the middle to late Caledonian, early Hercynian, late Hercynian, Indosinian, Yanshanian and Himalayan movements (Chen et al., 2019; He et al., 2013; Zhang et al., 2011a; Wu et al., 2020; Wu et al., 2016). The tp12cx fault experienced multistage tectonic movements and continued to move, retaining the signs of each stage of movement. Thus, the tp12cx fault is representative for studying the structural characteristics of each stage in the evolution of strike-slip faults in the Tarim Basin. Since the strike-slip fault zone played an important role in controlling the development of the Ordovician karst reservoir and hydrocarbon accumulation from the middle Caledonian to the early Hercynian period, this paper mainly discusses the segmentation characteristics of the strike-slip fault from the middle Caledonian to the early Hercynian and its control on hydrocarbon accumulation.

DATA AND METHODS

The data used in this paper include high-precision 3D seismic volume data, drilling logging data distributed along the fault zone, and drilling production data. The 3D seismic data are high-precision prestack depth migration data processed in Tahe

in 2020, with a total stacking area of 1600 km², bin of 15 m × 15 m, sampling rate of 1 m, and two-way travel time of 7 s. Drilling logging data are used to identify the seismic horizon, drilling vent and leakage segment to demarcate the fault boundary, and drilling production data are used to analyze the oil enrichment pattern.

The research ideas and methods are as follows: 1) Combined with the changes in the movement mode of the tp12cx strike-slip fault caused by regional stress changes, the structural evolution characteristics of the top of the Ordovician Yingshan Formation in the key structural period of the tp12cx strike-slip fault are restored. Based on the segmentation of the tp12cx strike-slip fault, the fault genetic segmentation types under the changes in movement mode are divided (Zhang et al., 2011b; Wu et al., 2016; Wu et al., 2020). 2) The width of each fault zone and drilling production of the tp12cx strike-slip fault are counted to verify the rationality of the genetic segmentation type. The distribution of strike-slip faults in key structural layers can be identified by the properties of coherence, tensor and dip angle. Since the northern part of tp12cx fault is a buried hill area jointly controlled by paleogeomorphology and faults, the role of fault in controlling reservoir is weakened compared with the southern covering area; thus, the width and nature of the fault zone in the fault-controlled karst area only in the southern part of the tp12cx fault are assessed. Among the faults, the top fault in the Ordovician Yingshan Formation dolomitic limestone (seismic reflection group T_7^6) is used to calculate the width of the fault zone to avoid the illusion of widening of the fault zone caused by dissolution. The width of the fault zone is determined by the ratio of the area of the fault zone to the approximate length of the fault zone. 3) The relationship between the genetic segmentation type and the reservoir is analyzed, and a corresponding reservoir model is established. First, using the root mean square amplitude change



rate attribute of the Ordovician Yijianfang Yingshan Formation is a relatively mature method (Ma et al., 2019; Wang et al., 2019) to predict the karst fracture vuggy reservoir in the study area. Through

the superposition of the strike-slip fault and fracture vuggy reservoir and the width of the fault zone, the impacts of the movement mode, genesis and segmentation type on the fracture vuggy reservoir are

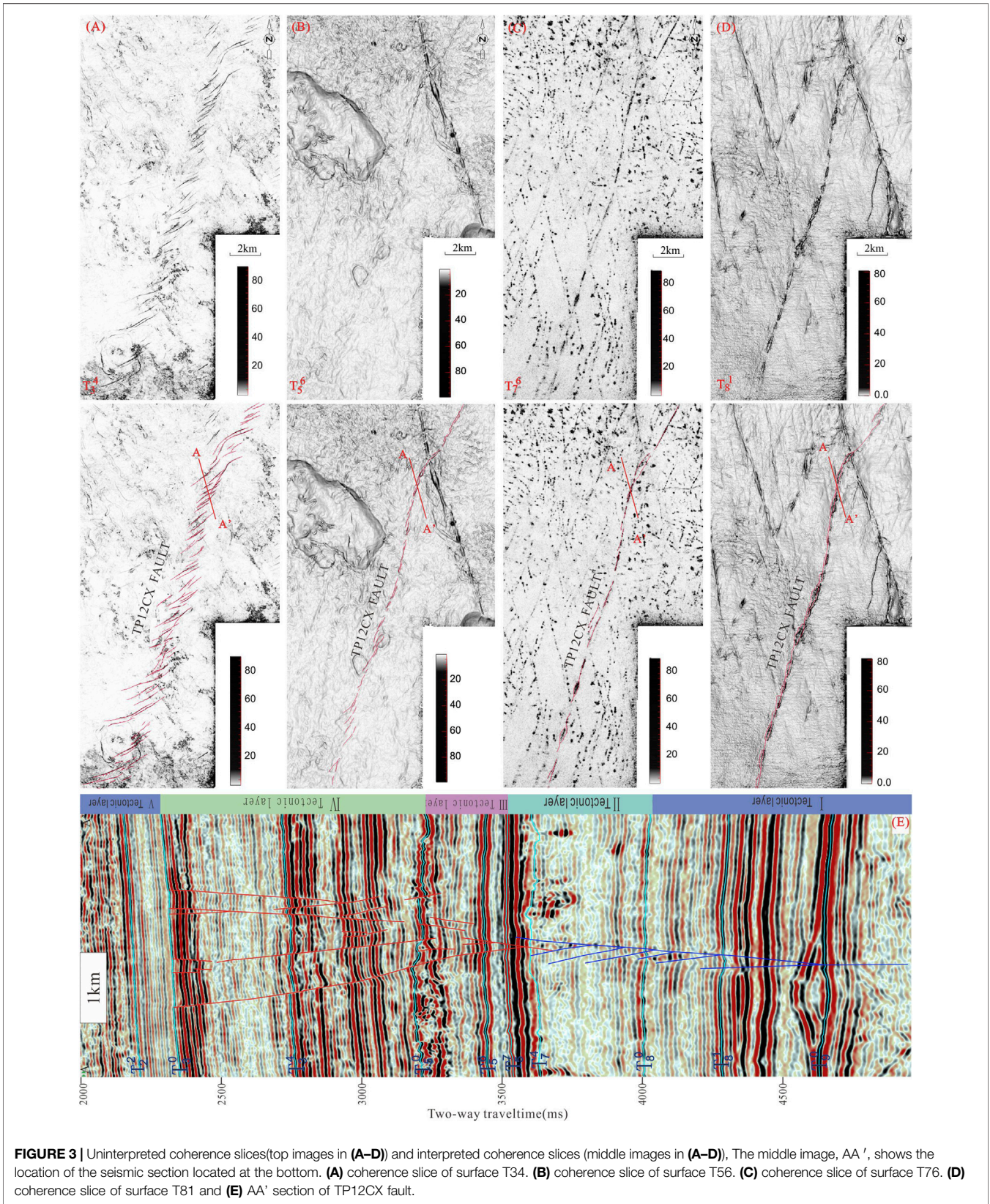
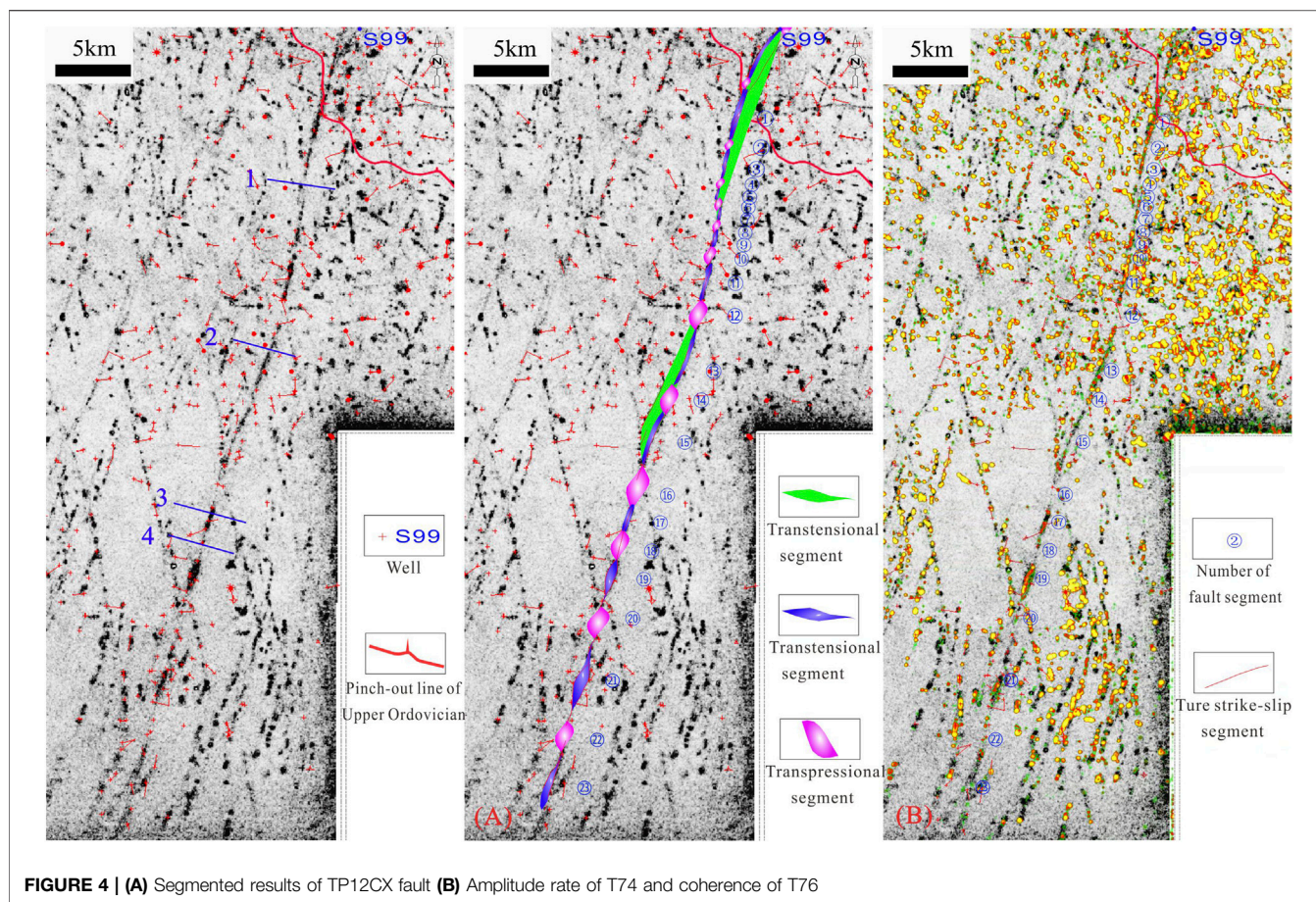


FIGURE 3 | Uninterpreted coherence slices(top images in (A–D)) and interpreted coherence slices (middle images in (A–D)). The middle image, AA', shows the location of the seismic section located at the bottom. (A) coherence slice of surface T34. (B) coherence slice of surface T56. (C) coherence slice of surface T76. (D) coherence slice of surface T81 and (E) AA' section of TP12CX fault.



analyzed. The second step is to analyze the differences in oil enrichment of the segmented types through drilling oil production and to establish the oil enrichment model corresponding to the genetically segmented types of Ordovician movement modes.

RESULTS

Structural Stratification

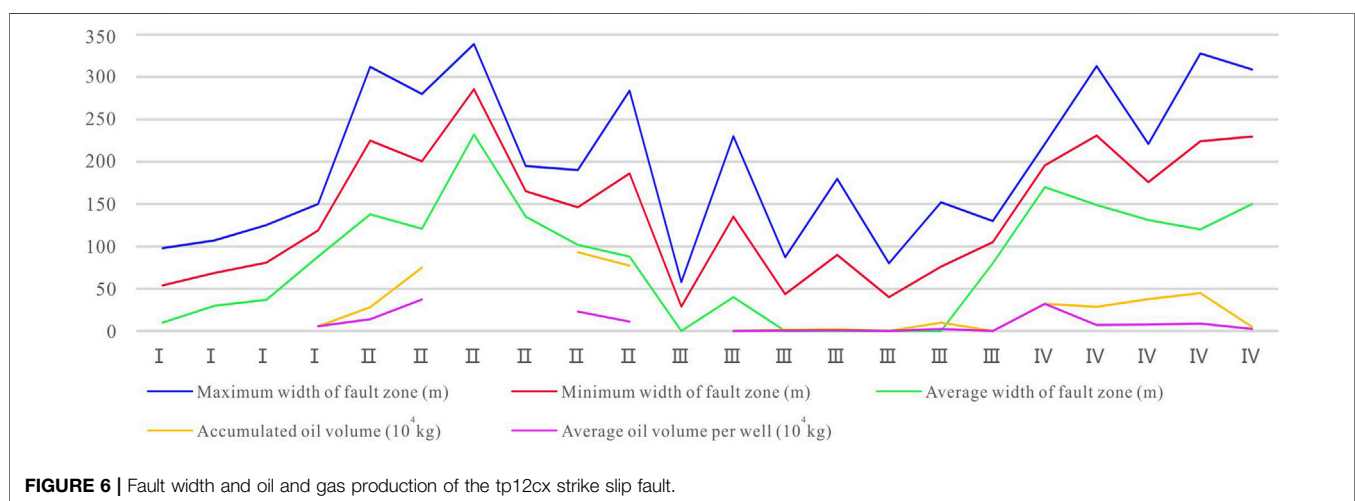
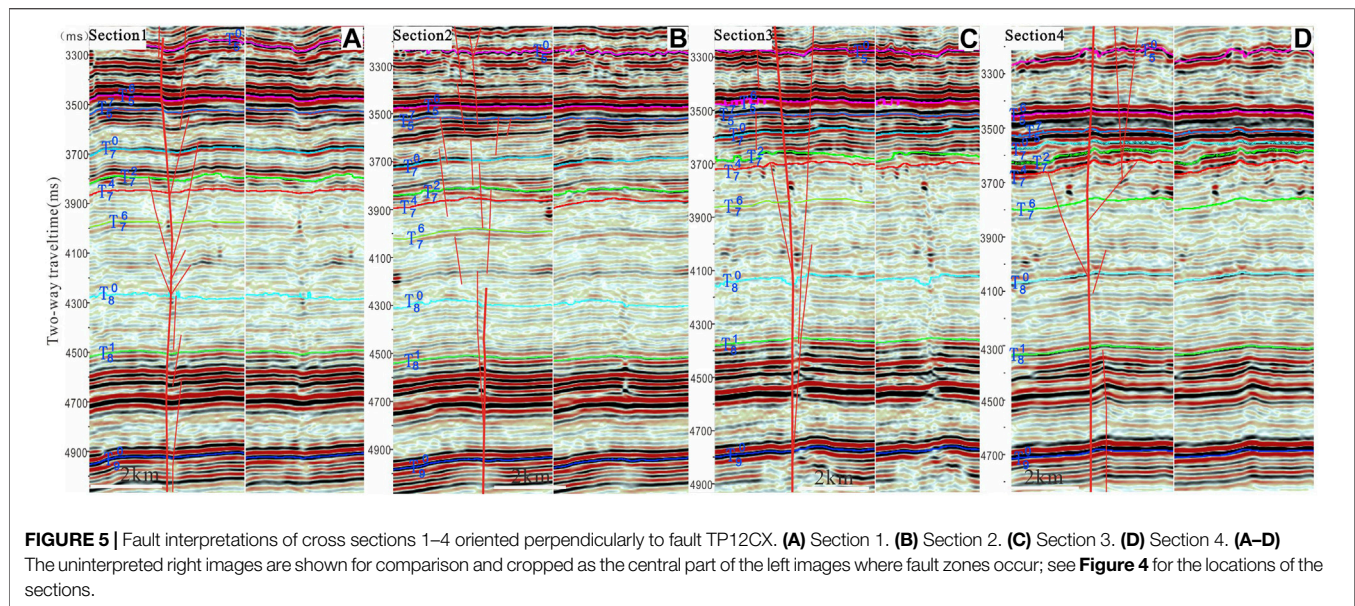
Vertically, the study area is divided into five structural layers (**Figure 3**). Structural layer I (E_{2a} ~ basement) developed normal faults. The second structural layer (D_{3d} ~ E_{2a}) is the most developed fault layer, which contains mainly NE-trending and NW-trending flower-like strike-slip faults. Some of the main NE- and NW-trending strike-slip faults of structural layer III (P ~ D_{3d}) continued to move. The fourth structural layer (P ~ E) consists of grabens and half-grabens controlled by tensional torsional left-lateral normal faults. In structural layer V (above E), faults are underdeveloped.

Geometry Characteristics of Fault

The TP12CX strike-slip fault zone can be divided into 23 segments, 12 segments of transtension segment, 11 segments of transpression segment (**Figure 4**) in mudstone covered area of The Sangtamu Formation, and the pure strike-slip segment is missing.

Transpression segment: fault anticlines or anticlines characterized by transpression in the segment (**Figures 5A,C**), which break down through the middle and lower Cambrian strata and spread upward in the face of T80 reflection layer to form fault anticlines or anticlines. Different degrees of faults are developed along the axis of the fault anticline, and the number and connectivity of faults are greatly different. Most of the seismic reflection characteristics are chaotic weak reflection, and the strong reflection of the string of beads is underdeveloped. There are strong reflections on the two wings of the fault anticline and continuous weak reflections on the two wings of the anticline. The reflection characteristics of faults are continuous downward, and the faults in the T80-T74 seismic reflection layer become discontinuous and appear intermittently. The number of faults is less than that of transtensional segmental faults, the fault grade is smaller and the connectivity between upper and lower faults is poor. The width of the fault zone ranges from 0 to 110m, and the oil production ranges from 0 to 57,300 tons (**Figure 6** and **Table 1**). **Figure 4B** shows the overall underdevelopment of the reservoir.

Transtension segment: the segment is characterized by vertical tensional half-graben or graben, and the fault zone is chaotic, beadlike strong reflection is generally developed, with high fracture degree and good connectivity above and below the fault (**Figures 5A,C**). In plane, the fault is rhomboid and



banded. Compared with the transpression segment, the number of faults is larger, and the connectivity between upper and lower faults is better. The width of the fault zone ranges from 110 to 345 m, with oil production ranging from 24,700 to 374,400 tons (**Figure 6** and **Table 1**). **Figure 4B** shows that the reservoir is more developed as a whole.

DISCUSSION

Tectonic Evolution of the tp12cx Fault in a Key Tectonic Period

Given the regional geological background of the Tabei uplift (Zhang et al., 2011a; Wu et al., 2020; Wu et al., 2016), the tp12cx fault mainly experienced the early Caledonian, middle to late Caledonian, early Hercynian, late Hercynian, Indosinian, Yanshanian and Himalayan movements. During these

movements, the NE-trending tp12cx strike-slip fault did not develop along the NE-trending (**Figure 2**) transtensional faults formed in the early Caledonian period, so the influence of tectonic activity in this period is not considered. The South Tianshan orogeny lasted until the end of the Triassic and then entered the postorogenic stress relaxation stage from the Jurassic to the Early Cretaceous. Regional tectonic transension occurred along the early large-scale strike-slip faults, forming a series of echelon left-step transtensional faults. Therefore, the influence of Indosinian and Yanshanian tectonic movements is not considered. This paper mainly focuses on the relationship between the movement mode transformation and fault segmentation of the (Wu et al., 2020) strike-slip fault in the middle to late Caledonian, early Hercynian and late Hercynian.

In the middle Caledonian stage I-III movements, the Tabei area was under the action of a N-S-trending compressive tectonic stress field, forming a series of NW- and NE-trending “X”-type

TABLE 1 | Characteristics and oil and gas production of each segment of the tp12cx strike slip fault.

Number of Fault Segment	Types of Fault Segments	Structural Properties	Maximum Width of Fault Zone (m)	Minimum Width of Fault Zone (m)	Average Width of Fault Zone (m)	Accumulated Oil Volume (10 ⁴ Kg)	Average Oil Volume per Well (10 ⁴ Kg)	Number of Wells
1	II	Extension	292	138	210	28.2	14.1	2
2	I	Compression	98	10	30	0	0	0
3	II	Extension	220	121	160	74.88	37.44	2
4	I	Compression	107	30	63	Reservoir nature reserve, unable to drill		
5	II	Extension	339	232	243			
6	I	Compression	125	37	82			
7	II	Extension	165	125	155			
8	III	Compression	58	0	14			
9	IV	Extension	251	200	219	32.23	32.23	1
10	III	Compression	230	40	110	0.23	0.23	1
11	IV	Extension	343	169	255	28.48	7.12	4
12	III	Compression	87	0	10	1.34	0.67	2
13	II	Extension	190	92	155	93	23.25	4
14	I	Compression	150	88	110	5.73	5.73	1
15	II	Extension	284	80	172	77.35	11.05	7
16	III	Compression	180	0	20	2.07	1.035	2
17	IV	Extension	225	138	180	37.79	7.558	5
18	IV	Compression	80	0	30	0	0	0
19	IV	Extension	442	120	345	44.81	8.962	5
20	III	Compression	152	0	40	10.02	2.505	4
21	IV	Extension	329	150	212	4.94	2.47	2
22	III	Compression	130	80	110	0	0	0
23	IV	Extension	320	150	275	80.18	11.45429	7

conjugate shear fault systems (**Figure 7A**). The NW-trending faults are dominated by right-lateral motion and left steps, while the NE-trending faults are dominated by left-lateral motion and left steps. The overlapping segments of the left step of the NW-trending fault are compressive. The overlapping segments of the left step of the NE-trending fault are mainly pulled apart, and the pure strike-slip segments are vertical linear faults.

From the late Caledonian to early Hercynian, under the NNE or NE shear stress produced by NW-SE transpression, the tp12cx fault moved again, and its mode changed from left-lateral to right-lateral strike-slip movement. The left-lateral and left-step faults, which resulted in the formation of early left-lateral strike-slip motion, disappeared in the process of right-lateral strike reverse strike-slip motion, and their formation and evolution experienced two stages. In the first stage (**Figure 7B**), the left-lateral left-step segment is transformed into a right-lateral left-step fault segment. The original left-step overlapping transtensional segment is undergoing pure strike-slip motion. In the process of right-lateral strike-slip movement, the left-step pure strike-slip segment is compressed and closes to form a positive flower-like deformation with transpressional uplift. In the second stage, with continuous right-lateral strike-slip activity, a regional arc-shaped right-lateral and right-step fault composed of several left-step faults forms (**Figure 7C**).

In the late Hercynian period, influenced by the southwestern Tarim orogenic belt, the tp12cx fault moved in the form of right-lateral motion under long-distance transpression from south to north. This interpretation further confirms that the arcuate faults

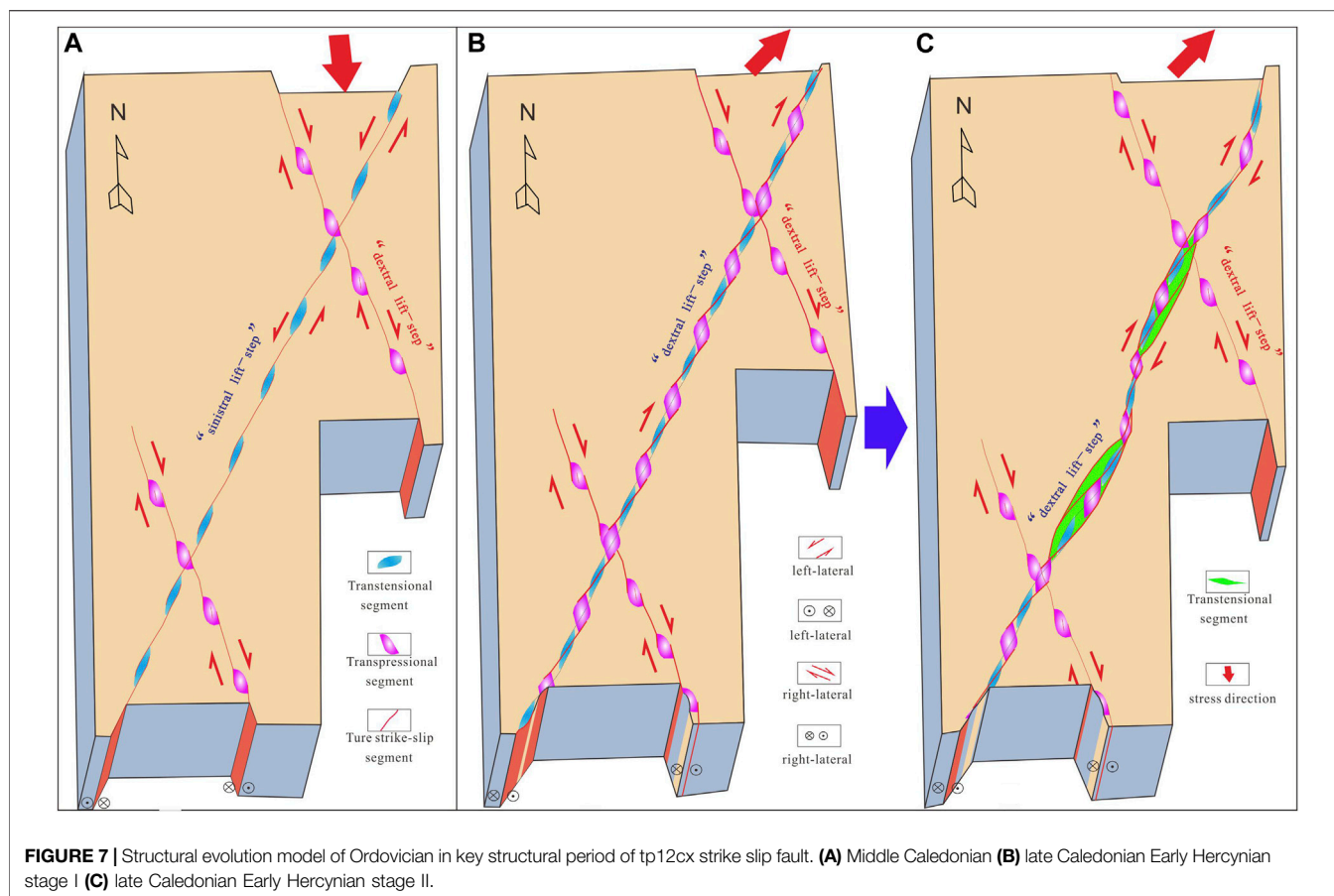
in the right-lateral right-step region include small left-lateral left-step faults.

Genetic Segmentation Type

From the above fault evolution characteristics, it can be seen that the segmented characteristics of TP12CX strike-slip faults are due to the transformation of fault motion mode, which leads to the continuous change of fault arrangement and fracture properties. The tp12cx strike-slip fault is divided into four genetic segmentation types according to the mutual superposition of overlapping segments and pure strike-slip segments, the change characteristics of fault properties, and the statistical data characteristics of reservoir development (**Figure 4**), drilling production data and fault width (**Table 1**).

Type I: left-step pure strike-slip segment + left-step transpressional segment + right-step transtensional segment.

In the middle Caledonian, this type of segment is a left-step pure strike-slip segment. From the late Caledonian to early Hercynian, after transformation from left-lateral to right-lateral strike-slip motion, this type of segment appears as a right-lateral and left-step overlapping segment, showing a positive flower-like structural style. Under the continuous action of right-lateral strike-slip motion, only a few more faults form in the transtensional zone of the right-lateral right-step segments in the region, and the pattern of normal flower transpression remains unchanged (**Figure 5B**, **Figure 8**). The fault breaks downward through the middle and lower Cambrian strata, displaces the anticline upward and deforms, with faults on both limbs and a few small faults on the axis of the anticline.



Against the background of disordered weak reflections, only beaded strong reflections are developed along the fault, the number of faults is small, and the width of the fault zone is 30–110 m. At least one well is drilled, and the average oil production capacity of each segment is 57300 tons. The average oil production of a single well is 57300 tons. The average oil production of a single well is equal to the ratio of the cumulative production sum to the sum of wells.

Type II: left-step transtensional segment + left-step pure strike-slip segment + right-step transtensional segment.

In the middle Caledonian, this type of segment is a left-step transtensional overlapping segment, and it then becomes a left-step pure strike-slip segment under the action of right-lateral strike-slip motion and still retains the negative flower-like structural style. Under the continuous action of right-lateral strike-slip, it is in the regional right-lateral and right-step transtensional zone, the number of faults increases, and the transtensional range is larger. The overall result is a rhombic and banded transtensional zone (Figures 5A, 8), which is broken up and down with a high degree of fragmentation. In the fault zone, disordered and beaded strong reflections are widely developed. The number of faults is the highest, and the width of the fault zone ranges from 110 to 243 m. The number of drilling wells is up to 11. The oil production capacity of each segment ranges from

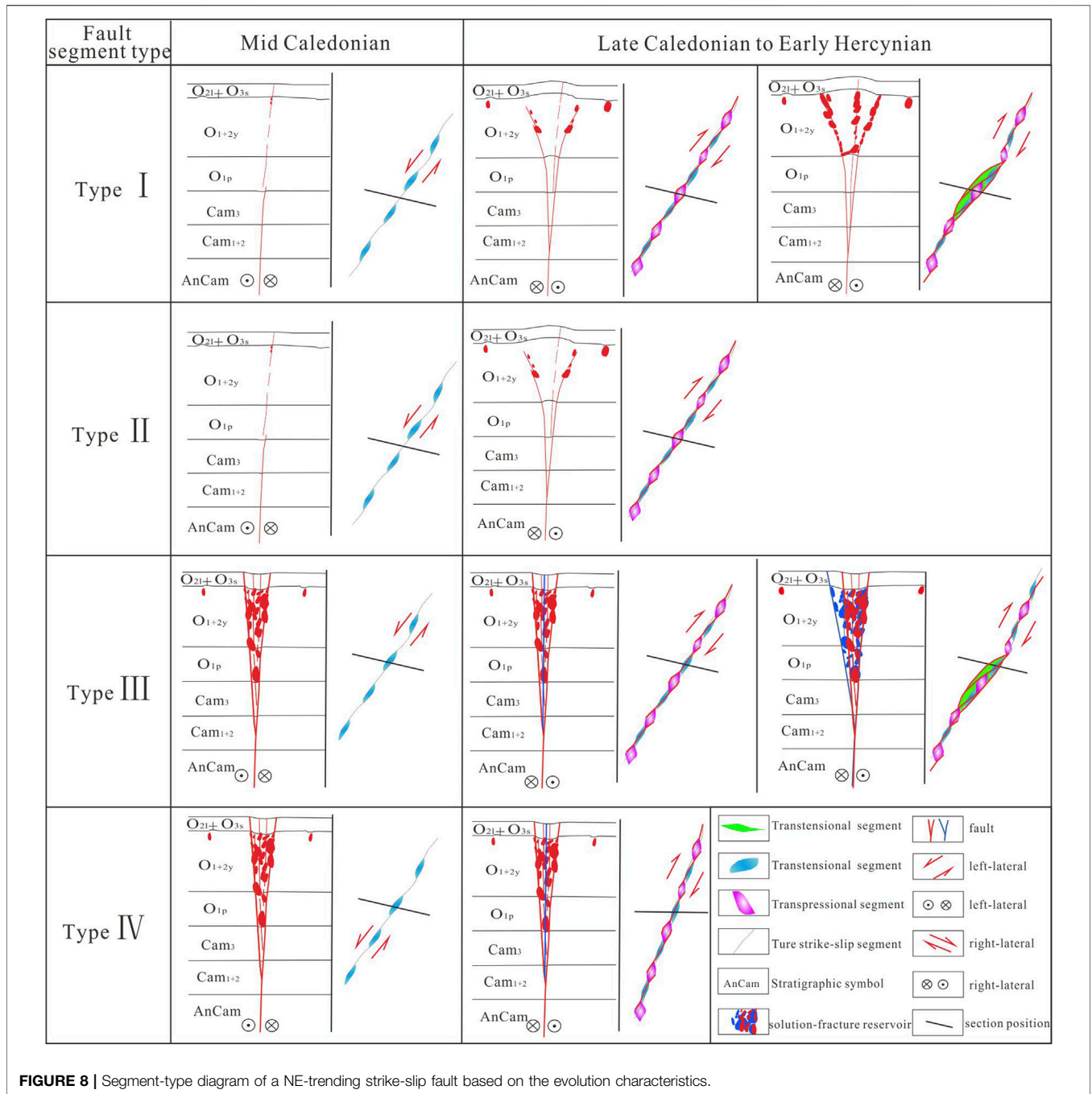
110500 to 374400 tons, and the average oil production of a single well is approximately 182300 tons.

Type III: left-step pure strike-slip segment + left-step transpressional segment + right-step pure strike-slip segment.

In the middle Caledonian period, this type of segment is a left-lateral left-step pure strike-slip segment, and a right-lateral strike-slip segment then becomes a right-lateral left-step overlapping segment, which is blocked in a transpression normal flower structure style (Figures 5D, 8). This type is very similar to type I, except that the axial fault of the anticline is underdeveloped and the strong reflection of the anticline is not developed. The number of faults is the lowest, the width of the fault zone is 0–80 m, and 9 wells are drilled. The oil production capacity of each segment is 0–25000 tons, and the average oil production of a single well is approximately 15200 tons. The benefit of a single well is low, and few wells are deployed.

Type IV: left-step transtensional segment + left-step pure strike-slip segment + right-step pure strike-slip segment.

In the middle Caledonian period, this type of segment is a left-lateral left-step transtensional overlap segment, and a right-lateral strike-slip segment then becomes a right-lateral left-step pure strike-slip segment, which still retains the negative flower-like structural style and is of transtensional nature as a whole (Figures 5C, 8). The target layer is characterized by



disordered strata, abundant strong seismic reflection anomalies, obvious fault extent and good communication between the upper and lower layers. The width of the fault zone is 180–345 m, and up to 23 wells have been drilled. The average oil production capacity of each segment is 24700–322300 tons, and the average oil production of a single well is approximately 95200 tons.

According to the statistical results (Figure 6), 1) the number of wells indicates that the regional right-lateral and right step transensional segment is only locally developed. 2) The number

of faults, the width of the fault zone, the size of the reservoir and the oil production in the transensional segment are larger than those in the transpressional segment. 3) The larger the number of faults and the width of the fault zone are, the larger the reservoir scale and oil production. 4) The width of the fault zone, reservoir scale and reservoir quality are ordered as type II > type IV > type I > type III. The reservoirs in the transpressional segment are developed along strike-slip faults on a large scale, and the reservoirs far from the fault zone are weakly developed. The fracture cavity bodies in the

transpression segment are scattered, isolated or undeveloped along the strike-slip fault zone.

Development Model of Fault-Solution Reservoir

The distribution and scale of Ordovician reservoirs in the tp12cx strike-slip fault zone are controlled by the segmentation type of strike-slip faults, and the segmentation type of strike-slip faults is controlled by the multistage superposition and transformation of overlapping and pure strike-slip segments caused by the movement mode of strike-slip faults.

In the middle Caledonian period, under the action of left-lateral strike-slip motion, left-step arranged strike-slip faults formed. The overlapping segment of the left step has the property of transtension, and the pure strike-slip segment is a vertical linear fault. Regardless of whether the number and width of faults in the transtension area of the overlapping segment are much larger than those in the pure strike-slip segment, the karstification and dissolution degree along the fault zone are much greater than those along the pure strike-slip segment, and the reservoir scale is correspondingly better than that along the pure strike-slip segment.

From the late Caledonian to the early Hercynian, the tp12cx fault reversed to right-lateral strike slip, and the original left lateral and left step fault styles were transformed. First, the arrangement of the left step fault did not change, but only the fault style and local properties changed. That is, the left step transtensional segment is most easily transformed as a weak zone due to more developed faults and fractures, a higher degree of fragmentation and a wider fault zone and is transformed into a right-lateral and left step pure strike-slip segment, retaining the transtensional property. Due to the vertical plane shape of the fault and weak fracture network fragmentation, the original left step pure strike-slip segment is not easily transformed by the later tectonic activities. Under the action of later tectonic activities, it gradually changes into a right lateral and left step overlapping area and forms a “positive” flower-shaped transpression segment of the fault anticline under the action of extrusion pressure. In the early stage, the scale of the karst stage and the right-lateral displacement fracture network are better, and the properties of the left and right displacement fractures are better preserved. In the right lateral and left step overlapping segment, the original fault is compressed and partially closed, and the fracture cave reservoir becomes worse. The two newly formed wing faults of the anticline experience karstification in this period and develop fracture cave reservoirs, and the scale of the reservoirs is relatively limited. Second, under the action of continuous right-lateral strike slip, the bending effect occurs, and a regional arc right-lateral strike-slip fault is gradually formed. The interior is composed of faults arranged on the left step. The overlapping segment of the right lateral and right step in the region is generally weakly pulled apart, and the number, width and reservoir development scale of faults in the transpression segments and transtension segments are relatively better than those in the pure strike-slip segments. Among them, the number and degree of fractures in the transtension segments of the left step are greater,

the karstification is stronger, and the reservoir is more developed. The transpression segment is compacted, the faults on both wings of the anticline are opened, the karstification becomes stronger, and the reservoir becomes better. Since the late Hercynian karstification has made little contribution to the Ordovician carbonate cave reservoir, the fractured reservoir formed by the fault itself has limited reservoir capacity (Zhang et al., 2011b; Zhou et al., 2011a; Zhang et al., 2012; Han et al., 2016). The right lateral and right step overlapping transtension segment, regardless of the reservoir scale and reservoir scale, is larger than the right lateral and right step pure strike-slip segment. The main reservoir-forming period in the study area was the late Caledonian Indosinian period (Zhu et al., 2010), indicating that the regional arc right lateral and right step strike-slip faults formed before the late Hercynian period, and the reservoir scale was controlled by the pre-Hercynian correlation.

It can be seen from the above that the scale of the reservoir is jointly controlled by the number and nature of faults and corresponding karstification, but the strength of karstification is controlled by the segmented type of strike-slip faults. Therefore, in the final analysis, the scale of the reservoir is controlled by the number and nature of strike-slip faults, especially the nature of strike-slip faults.

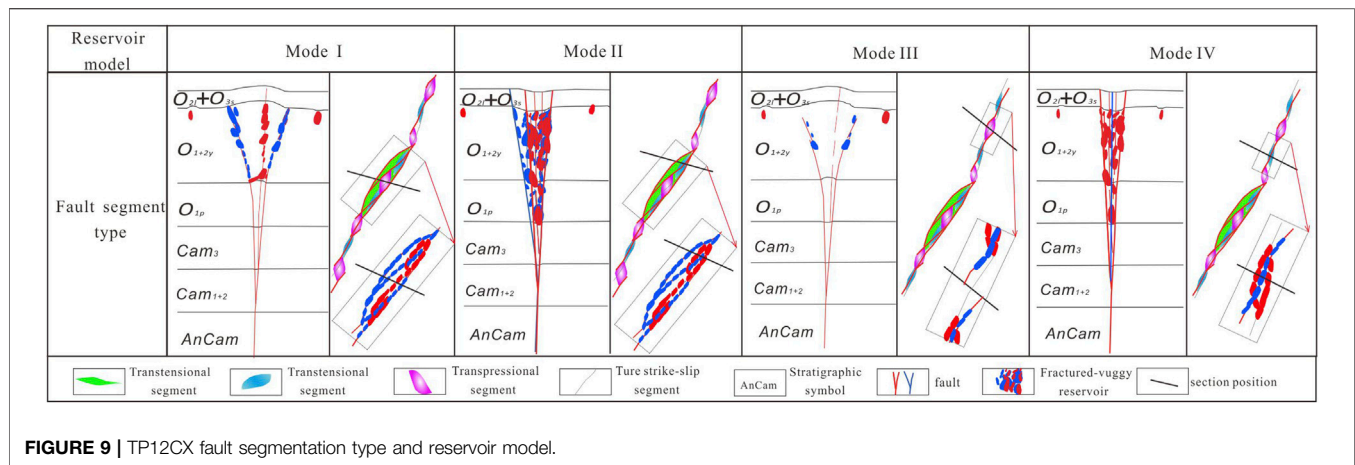
Fault Solution Reservoir Model

The structure of the fault fracture network and matched karst reservoir jointly determine the development characteristics of the reservoir. Four types of strike-slip fault segments correspondingly form four types of fault solution reservoir models (Figure 9):

Type I reservoir model, corresponding to the type I structure. The evolution process of fault properties is first transpression, then transtension. The whole area is characterized by fault anticline transpression, obvious fault distance in the deep part, positive flower-shaped fault anticline deformation in the shallow part, and beaded strong reflection reservoirs developed along the two wings and axis faults of the anticline. After the left-lateral changes to right-lateral strike slip, it translates and slides in the formed left-lateral strike-slip zone, and then the sliding in the left-lateral strike-slip segment is blocked to form a flower-shaped fault anticline and then form a regional right-lateral strike-slip fault. This stress gradient transmission mode does not make the whole fault anticline disappear; that is, the scale of the bending effect in the late stage is small, which is not enough to change the whole right-lateral strike-slip segment into an transtension zone. Only the faults and fractures are more developed, the reservoir connectivity is better, and the reservoir scale is better than that of the type III extrusion segment. The average oil production of a single well is lower, reaching 57300 tons.

Type II reservoir model, corresponding to the type II structure type. The evolution process of fault properties is: first transtension, then transtension. A wide graben is formed by vertical faults as a whole. The plane is in a continuous banded and rhombic shape. The fault width is large. The beaded strong reflection reservoir is developed along the whole fault zone. The average oil production of a single well is the largest, up to 182300 tons.

The reservoir model of the type III segment corresponds to the type III structure type. and the evolution of fault properties has



only experienced transpression. It is very similar to the type I transpression mode, but the difference is that the anticline axis fault is underdeveloped, and the beaded strong reflection reservoir is also underdeveloped. The average oil production of this type of single well is the lowest, only 15200 tons. This is because this type of segment is a translational segment in the middle Caledonian period, and karstification developed along the line-like faults. Under the action of transpression and torsion from the late Caledonian to the early Hercynian, the lithology was dense, and the physical properties of the original reservoir worsened. At the same time, the weak faults along the two wings of the anticline were dissolved to form a limited reservoir with a small scale.

Type IV reservoir model, corresponding to the type IV reservoir structure. The evolution of fracture properties only experienced tension. Narrow symmetrical grabens or asymmetric half grabens are formed by vertical faults, with relatively continuous linear planes and narrow widths. Strong amplitude reflection reservoirs are developed along the whole fault zone. The average oil production of a single well is more than once, reaching 95200 tons.

CONCLUSION

The tp12cx strike-slip fault experienced two key stages of tectonic movement determining segmentation: middle Caledonian and late Caledonian to early Hercynian. In the middle Caledonian period, right-lateral and right-step faults form. The overlapping left-step segment is a transensional zone, and the remainder is a linear pure strike-slip segment. From the late Caledonian to early Hercynian, the mode changes from left-lateral strike-slip to right-lateral strike-slip movement. The left-step tension fracture zone first ruptures and retains the property of being transensional, while the left-step linear pure strike-slip segment is transformed into a left-step overlapping segment with

transpression. With continuous right-lateral movement, a regional right-lateral right-step strike-slip fault composed of several left-step faults is formed.

Four structure types of strike-slip faults and corresponding reservoir models are divided based on the structural evolution process. The left-step pure strike-slip segment + left-step transensional segment + right-step transensional segment is type I, the left-step transensional segment + left-step pure strike-slip segment + right-step transensional segment is type II, the right-step translation + left-step pure strike-slip segment left-step pure strike-slip segment + left-step transensional segment is type III, and the left-step transensional segment + left-step pure strike-slip segment is type IV. The fault width and oil production of type II and type IV fractures with transensional properties are much larger than those of transpression types I and III.

DATA AVAILABILITY STATEMENT

The original contributions presented in the study are included in the article/Supplementary Material, further inquiries can be directed to the corresponding author.

AUTHOR CONTRIBUTIONS

YL: Provide research ideas; HM: The structural analysis and genetic type of TP12cx strike-slip fault are summarized; ZW: Reservoir type summary and analysis; GD: Statistical analysis of data; HW: Statistical analysis and mapping of data.

ACKNOWLEDGMENTS

We thank all editors and reviewers for their helpful comments and suggestions.

REFERENCES

- Aydin, A., and Nur, A. (1982). Evolution of Pull-Apart Basins and Their Scale Independence. *Tectonics* 1 (1), 91–105. doi:10.1029/tc001i001p00091
- Aydin, A., and Nur, A. The Types and Role of Steppers in Strike-Slip Tectonics. 1985, 37:35–44. doi:10.2110/pec.85.37.0035
- Chemenda, A. I., Cavalié, O., Vergnolle, M., Bouissou, S., and Delouis, B. (2016). Numerical Model of Formation of a 3-D Strike-Slip Fault System. *Comptes Rendus Geosci.* 348 (1), 61–69. doi:10.1016/j.crte.2015.09.008
- Chen, G. B., Li, T., and Yang, L. (2021). Mechanical Properties and Failure Mechanism of Combined Bodies with Different Coal-Rock Ratios and Combinations. *J. Min. Strata Control Eng.* 3 (2), 023522. doi:10.13532/j.jmsce.cn10-1638/td.20210108.001
- Chen, J. J., He, D. F., and Sun, F. Y. (2019). Three Dimensional Geological Structure of Tabei Paleouplift and Related Problems. *Geosci. Front.* 26 (01), 121–133. doi:10.13745/j.esf.sf.2019.1.8
- Cunningham, W. D., and Mann, P. (2007). Tectonics of Strike-Slip Restraining and Releasing Bends. *Geol. Soc. Lond. Spec. Publ.* 290 (1), 1–12. doi:10.1144/sp290.1
- Davis, G. H., Bump, A. P., Garcia, P. E., and Ahlgren, S. G. (2000). Conjugate Riedel Deformation Band Shear Zones. *J. Struct. Geol.* 22 (2), 169–190. doi:10.1016/S0191-8141(99)00140-6
- de Jossineau, G., and Aydin, A. (2007). The Evolution of the Damage Zone with Fault Growth in Sandstone and its Multiscale Characteristics. *John Wiley Sons, Ltd* 112 (B12), 6. doi:10.1029/2006jb004711
- Deng, S., Li, H., Zhang, Z., Zhang, J., and Yang, X. (2018). Structural Characterization of Intracratonic Strike-Slip Faults in the Central Tarim Basin. *AAPG Bull.* 103 (1)109-137. doi:10.1306/06071817354
- Deng, S., Liu, Y. Q., and Liu, J. (2021). Development and Evolution of Strike Slip Faults in the Inner Craton Basin and Their Petroleum Geological Significance: a Case Study of Shunbei Area. *Tarim Basin. Geotect. metallogeny*, 1–16. [2021-05-15]. doi:10.16539/j.ddgzycx
- Dooley, T. P., and Schreurs, G. (2012). Analogue Modelling of Intraplate Strike-Slip Tectonics: A Review and New Experimental Results. *Tectonophysics* 574-575, 1–71. doi:10.1016/j.tecto.2012.05.030
- Fan, C., Li, H., Qin, Q., He, S., and Zhong, C. (2020). Geological Conditions and Exploration Potential of Shale Gas Reservoir in Wufeng and Longmaxi Formation of Southeastern Sichuan Basin, China. *J. Petroleum Sci. Eng.* 191, 107138. doi:10.1016/j.petrol.2020.107138
- Han, C. C., Lin, C. Y., and Ren, L. H. (2016). Characteristics of Ordovician Fault in the Block 10 of Tahe Oilfield, Tarim Basin and its Controlling Effect on Karst Reservoirs. *Nat. Gas. Geosci.* 27 (5), 790–798. doi:10.11764/j.issn.1672-1926.2016.05.0790
- He, B. Z., Jiao, C. L., and Xu, Z. Q. (2013). Response of Tectonic Unconformity in the Middle Late Caledonian Period of Tarim Basin to the Tectonism of Peripheral Orogenic Belt. *Acta Geol. Sin.* 87 (S1), 34. doi:10.1111/1755-6724.12148_4
- He, X., Zhang, P., He, G., Gao, Y., Liu, M., Zhang, Y., et al. (2020). Evaluation of Sweet Spots and Horizontal-Well-Design Technology for Shale Gas in the Basin-Margin Transition Zone of Southeastern Chongqing, SW China. *Energy Geosci.* 1 (3–4), 134–146. doi:10.1016/j.engeos.2020.06.004
- Hong, D., Cao, J., Wu, T., Dang, S., Hu, W., and Yao, S. (2020). Authigenic Clay Minerals and Calcite Dissolution Influence Reservoir Quality in Tight Sandstones: Insights from the Central Junggar Basin, NW China. *Energy Geosci.* 1 (1–2), 8–19. doi:10.1016/j.engeos.2020.03.001
- Jiang, T. W., Han, J. F., Wu, G. H., Yu, H., Su, Z., Xiong, C., et al. (2020). Differences and Controlling Factors of Composite Hydrocarbon Accumulations in the Tazhong Uplift, Tarim Basin, NW China. *Petroleum Explor. Dev. Online* 47 (2): 229-241. doi:10.1016/S1876-3804(20)60042-8
- Kim, Y.-S., Peacock, D. C. P., and Sanderson, D. J. (2003). Mesoscale Strike-Slip Faults and Damage Zones at Marsalforn, Gozo Island, Malta. *J. Struct. Geol.* 25 (5), 793–812. doi:10.1016/S0191-8141(02)00200-6
- Lan, S. R., Song, D. Z., Li, Z. L., and Liu, Y. (2021). Experimental Study on Acoustic Emission Characteristics of Fault Slip Process Based on Damage Factor. *J. Min. Strata Control Eng.* 3 (3), 033024. doi:10.13532/j.jmsce.cn10-1638/td.20210510.002
- Li, H., Qin, Q., Zhang, B., Ge, X., Hu, X., Fan, C., et al. (2020). Tectonic Fracture Formation and Distribution in Ultradeep Marine Carbonate Gas Reservoirs: A Case Study of the Maokou Formation in the Jiulongshan Gas Field, Sichuan Basin, Southwest China. *Energy fuels.* 34 (11), 14132–14146. doi:10.1021/acs.energyfuels.0c03327
- Li, H. (2022). Research Progress on Evaluation Methods and Factors Influencing Shale Brittleness: A Review. *Energy Rep.* 8, 4344–4358. doi:10.1016/j.egyr.2022.03.120
- Li, H., Tang, H., Qin, Q., Zhou, J., Qin, Z., Fan, C., et al. (2019). Characteristics, Formation Periods and Genetic Mechanisms of Tectonic Fractures in the Tight Gas Sandstones Reservoir: A Case Study of Xujiache Formation in YB Area, Sichuan Basin, China. *J. Petroleum Sci. Eng.* 178, 723–735. doi:10.1016/j.petrol.2019.04.007
- Li, W., Meng, M. F., and Chen, X. P. (2021). Quantitative Characterization of Extension and Compression Derived from Bending Strike Slip Faults in the Eastern Bohai Sea Area and its Petroleum Geological Significance. *J. China Univ. Petroleum Nat. Sci. Ed.* 45 (05), 23–32.
- Li, X. W., Feng, X. K., and Liu, Y. L. (2018). Anatomy of Ordovician Strike Slip Fault System and Analysis of its Reservoir Controlling Characteristics in Tazhong Area. *Pet. Geophys. Prospect.* 57 (05), 764–774.
- Li, Y., Zhou, D., Wang, W., Jiang, T., and Xue, Z. (2020). Development of Unconventional Gas and Technologies Adopted in China. *Energy Geosci.* 1 (1–2), 55–68. doi:10.1016/j.engeos.2020.04.004
- Liu, J., Yang, H., Xu, K., Wang, Z., Liu, X., Cui, L., et al. (2022). Genetic Mechanism of Transfer Zones in Rift Basins: Insights from Geomechanical Models. *GSA Bull.*, doi:10.1130/B36151.1
- Lu, X. B., Rong, Y. S., and Li, X. B. (2017). Injection Production Well Pattern Construction and Development Significance of Carbonate Fractured Vuggy Reservoir: a Case Study of Tahe Oilfield. *Petroleum Nat. gas Geol.* 38 (04), 658–664. doi:10.11743/ogg20170403
- Lu, X. B., Wang, Y., Tian, F., Li, X., Yang, D., Li, T., et al. (2017). New Insights into the Carbonate Karstic Fault System and Reservoir Formation in the Southern Tahe Area of the Tarim Basin. *Mar. Petroleum Geol.* 86: 587-605. doi:10.1016/j.marpetgeo.2017.06.023
- Lu, X. B., Yang, M., and Wang, Y. (2018). Characteristics of "stratabound" and "fault Controlled" Reservoirs in Northern Tarim Basin: a Case Study of Ordovician Reservoirs in Tahe Oilfield. *Pet. Exp. Geol.* 40 (04), 461–469.
- Ma, D. B., Tong, G. H., and Zhu, Y. F. (2019). Segmentation Characteristics of Deep Strike-Slip Faults in Tarim Basin and Their Control on Oil and Gas Enrichment: Taking Ordovician Strike-Slip Faults in Halahatang Oilfield in Tabei Area as an Example. *Earth Sci. Front.* 26 (01), 225–237.
- McClay, K., and Massim Bonora, M. (2001). Analog Models of Restraining Steppers in Strike-Slip Fault Systems. *Aapg Bull.* 85 (2), 233–260. doi:10.1306/8626c7ad-173b-11d7-8645000102c1865d
- Mitchell, T. M., and Faulkner, D. R. (2009). The Nature and Origin of Off-Fault Damage Surrounding Strike-Slip Fault Zones with a Wide Range of Displacements: A Field Study from the Atacama Fault System, Northern Chile. *J. Struct. Geol.* 31 (8), 802–816. doi:10.1016/j.jsg.2009.05.002
- Neng, Y., Yang, H. J., and Deng, X. L. (2018). Structural Patterns of Fault Damage Zones in Carbonate Rocks and Their Influences on Petroleum Accumulation in Tazhong Paleouplift, Tarim Basin, NW China. *Petroleum Explor. Dev. Online* 45 (1). doi:10.1016/S1876-3804(18)30004-1
- Qie, L., Shi, Y. N., and Liu, J. G. (2021). Experimental Study on Grouting Diffusion of Gangue Solid Filling Bulk Materials. *J. Min. Strata Control Eng.* 3 (2), 023011. doi:10.13532/j.jmsce.cn10-1638/td.20210111.001
- Qiu, H. B., Deng, S., Cao, Z., Yin, T., and Zhang, Z. (2019). The Evolution of the Complex Anticlinal Belt with Crosscutting Strike-Slip Faults in the Central Tarim Basin, NW China. *Tectonics* 38 (6), 2087–2113. doi:10.1029/2018TC005229
- Ramadhan, Aldis., Samudra, A. B., Puji Lestari, E., Saputro, J., Hirosiadi, Y., and Amrullah, I. (2018). Strike-Slip Fault Deformation and its Control in Hydrocarbon Trapping in Ketaling Area, Jambi Subbasin, Indonesia. *IOP Conf. Ser. Earth Environ. Sci.* 132 (1). doi:10.1088/1755-1315/132/1/012025
- Shan, S. C., Wu, Y. Z., Fu, Y. K., and Zhou, P. H. (2021). Shear Mechanical Properties of Anchored Rock Mass under Impact Load. *J. Min. Strata Control Eng.* 3 (4), 043034. doi:10.13532/j.jmsce.cn10-1638/td.20211014.001
- Stefanov, Y. P., and Bakeev, R. A. (2014). *Deformation and Fracture Structures in Strike-Slip Faulting*. Engineering Fracture Mechanics, 129, 102–111. doi:10.1016/j.engfracmech.2014.05.019

- Swanson, M. T. (2005). Geometry and Kinematics of Adhesive Wear in Brittle Strike-Slip Fault Zones. *J. Struct. Geol.* 27, 871–887. doi:10.1016/j.jsg.2004.11.009
- Wang, Y. T., and Li, J. L. (1999). Related Structures of Strike Slip Faulting. *Geol. Sci. Technol. Inf.* (03), 30–34.
- Wang, Z., Wen, H., Deng, G., Ding, W., and Wang, X. (2019). Fault-karst Characterization Technology in the Tahe Oilfield, China. *Geophys. Prospect. Petroleum* 58 (1), 149–154. doi:10.3969/j.issn.1000-1441.2019.01.017
- Wu, G. H., Kim, Y.-S., Su, Z., Yang, P., Ma, D., and Zheng, D. (2020). Segment Interaction and Linkage Evolution in a Conjugate Strike-Slip Fault System from the Tarim Basin, NW China. *Mar. Petroleum Geol.*, 112. doi:10.1016/j.marpetgeo.2019.104054
- Wu, G. H., Yang, H. J., He, S., et al. (2016). Effects of Structural Segmentation and Faulting on Carbonate Reservoir Properties: A Case Study from the Central Uplift of the Tarim Basin, China. *Mar. Petroleum Geol.*, 71. doi:10.1016/j.marpetgeo.2015.12.008
- Yin, S., and Ding, W. L. (2019). Evaluation Indexes of Coalbed Methane Accumulation in the Strong Deformed Strike-Slip Fault Zone Considering Tectonics and Fractures: A 3D Geomechanical Simulation Study. *Geol. Mag.* 156 (6), 1–17. doi:10.1017/s0016756818000456
- Yin, S., Dong, L., Yang, X., and Wang, R. (2020). Experimental Investigation of the Petrophysical Properties, Minerals, Elements and Pore Structures in Tight Sandstones. *J. Nat. Gas Sci. Eng.* 73, 1–14. doi:10.1016/j.jngse.2020.103189
- Yin, S., and Gao, Z. (2019). Numerical Study on the Prediction of "sweet Spots" in a Low Efficiency-Tight Gas Sandstone Reservoir Based on a 3D Strain Energy Model. *IEEE Access* 7 (6), 1–12. doi:10.1109/access.2019.2933450
- Yin, S., Lv, D. W., and Ding, W. L. (2018b). New Method for Assessing Microfracture Stress Sensitivity in Tight Sandstone Reservoirs Based on Acoustic Experiments. *Int. J. Geomechanics* 18 (4), 1–16. doi:10.1061/(asce)gm.1943-5622.0001100
- Yin, S., and Wu, Z. (2020). Geomechanical Simulation of Low-Order Fracture of Tight Sandstone. *Mar. Petroleum Geol.* 100, 1–16. doi:10.1016/j.marpetgeo.2020.104359
- Yin, S., Xie, R., Wu, Z., Liu, J., and Ding, W. (2019). *In Situ* stress Heterogeneity in a Highly Developed Strike-Slip Fault Zone and its Effect on the Distribution of Tight Gases: A 3D Finite Element Simulation Study. *Mar. Petroleum Geol.* 99 (1), 75–91. doi:10.1016/j.marpetgeo.2018.10.007
- Yin, S., Zhao, J., Wu, Z., and Ding, W. (2018a). Strain Energy Density Distribution of A Tight Gas Sandstone Reservoir In A Low-Amplitude Tectonic Zone And Its Effect On Gas Well Productivity: A 3D Fem Study. *J. Petroleum Sci. Eng.* 170, 89–104. doi:10.1016/j.petrol.2018.06.057
- Zhang, X. B., Lv, H. T., and Zhao, X. K. (2011a). Paleostuctural Evolution of Lower-Middle Ordovician Top and its Relationship with Hydrocarbon in Tahe Oilfield. *Petroleum Geol. Exp.* 33 (3), 233–238.
- Zhang, X. B., Lv, H. T., and Zhao, X. K. (2011b). Paleotectonic Evolution and Oil-Gas Relationship at the Top of Middle Lower Ordovician in Tahe Oilfield. *Pet. Exp. Geol.* 33 (03), 233–238.
- Zhang, X. F., Li, M., and Chen, Z. Y. (2012). Characteristics and Karstification of the Ordovician Carbonate Reservoir, Halahatang Area, Northern Tarim Basin. *Acta Petrol. Sin.* 28 (3), 815–826.
- Zhang, Z. P., Kang, Y., Lin, H., Han, J., Zhao, R., Zhu, X., et al. (2021). A Study on the Reservoir Controlling Characteristics and Mechanism of the Strike Slip Faults in the Northern Slope of Tazhong Uplift, Tarim Basin, China. *Arabian J. Geosciences* 14 (8). doi:10.1007/s12517-021-07076-5
- Zhao, K. K., Jiang, P. F., and Feng, Y. J. (2021). Investigation of the Characteristics of Hydraulic Fracture Initiation by Using Maximum Tangential Stress Criterion. *J. Min. Strata Control Eng.* 3 (2), 023520. doi:10.13532/j.jmsce.cn10-1638/td.20201217.001
- Zhao, R., Deng, S., Yun, L., Lin, H., Zhao, T., Yu, C., et al. (2020). Description of the Reservoir along Strike-Slip Fault Zones in China T-Sh Oilfield, Tarim Basin. *Carbonates Evaporites* 36 (1). doi:10.1007/s13146-020-00661-x
- Zheng, H., Zhang, J., and Qi, Y. (2020). Geology and Geomechanics of Hydraulic Fracturing in the Marcellus Shale Gas Play and Their Potential Applications to the Fuling Shale Gas Development. *Energy Geosci.* 1 (1–2), 36–46. doi:10.1016/j.engeos.2020.05.002
- Zhou, B. W., Chen, H. H., and Yun, L. (2022). Relationship between Fault Offset Segmentation Difference and Fault Width of Lower Paleozoic Strike Slip Fault Zone in Shunbei Area of Tarim Basin. *Earth Sci.* 47 (02), 437–451.
- Zhou, W., Li, X. H., and Jin, W. H. (2011). The Control Action of Fault to Paleokarst in View of Ordovician Reservoir in Tahe Area. *Acta Petrol. Sin.* 27 (8), 2339–2348.
- Zhu, G. Y., Yang, H. J., and Zhu, Y. F. (2010). Study on Petroleum Geological Characteristics and Accumulation of Carbonate Reservoirs in Hanilcatam Area, Tarim Basin. *Acta Petrol. Sin.* 27 (3), 827–844.
- Zhu, Q. Y., Dai, J., Yun, F. F., Zhai, H. H., Zhang, M., and Feng, L. R. (2022). Dynamic Response and Fracture Characteristics of Granite under Microwave Irradiation. *J. Min. Strata Control Eng.* 4 (1), 019921. doi:10.13532/j.jmsce.cn10-1638/td.20210926.001

Conflict of Interest: YL, HM, ZW, GD, and HW were employed by Sinopec Northwest Oilfield Company.

The author declares that the research was conducted in the absence of any commercial or financial relationships that could be construed as a potential conflict of interest.

Publisher's Note: All claims expressed in this article are solely those of the authors and do not necessarily represent those of their affiliated organizations, or those of the publisher, the editors and the reviewers. Any product that may be evaluated in this article, or claim that may be made by its manufacturer, is not guaranteed or endorsed by the publisher.

Copyright © 2022 Lv, Ma, Wang, Deng and Wen. This is an open-access article distributed under the terms of the Creative Commons Attribution License (CC BY). The use, distribution or reproduction in other forums is permitted, provided the original author(s) and the copyright owner(s) are credited and that the original publication in this journal is cited, in accordance with accepted academic practice. No use, distribution or reproduction is permitted which does not comply with these terms.